A R C H I V E S O F M E T A L L U R G Y A N D M A T E R I A L S
Volume 57 2012 Issue 3
DOI: 10.2478/v10172-012-0093-5

O. ZGALAT-LOZYNSKYY*, M. HERRMANN**, A. RAGULYA*, M. ANDRZEJCZUK***, A. POLOTAI****

STRUCTURE AND MECHANICAL PROPERTIES OF SPARK PLASMA SINTERED TiN-BASED NANOCOMPOSITES

STRUKTURA I WŁAŚCIWOŚCI MECHANICZNE NANOKOMPOZYTÓW NA BAZIE TiN SPIEKANYCH ISKROWO PLAZMOWO

Consolidation of commercially available titanium nitride nanostructured powder as well as nanocomposite powders in the Si_3N_4-TiN and TiN-TiB_2 systems have been performed by Spark Plasma Sintering (SPS) in the temperature range from 1200°C to 1550°C. The effect of non-linear heating and loading regimes on high melting point nanocomposites consolidation has been investigated.

Keywords: nanocomposites, Spark Plasma Sintering, Grain Boundaries, nanohardness

Spiekanie komercyjnego nanoproszku TiN jak i nanokompozytowych proszków Si_3N_4-TiN i TiN-TiB_2 zostało przeprowadzone metodą spiekania iskrowo plazmowego (SPS) w zakresie temperatur od 1200°C to 1550°C. Badano wpływ nieliniowego ogrzewania i warunków obciążenia na spiekanie wysokotopliwych nanokompozytów.

1. Introduction

Advanced carbides, borides and nitrides form a class of non-oxide ceramic compounds possessing important properties such as high melting point, extremely high hardness and wear resistance, low specific gravity, as well as retain mechanical properties and chemical stability at high temperatures. Such unique combination of properties makes non-oxide materials extremely valuable for applications in aerospace, nuclear and mining industries, and also for armour and cutting tools. Further improvement of mechanical properties is possible by decreasing grain size in the compositions to the nanometer scale (less than 100nm), exploring so called "size effect" – rise of hardness and bending strength with decreasing of grain size.

Spark Plasma Sintering (SPS) is a special very fast hot pressing method with a direct heating of the die or the powder compact by a pulsed direct current. One of the SPS features is a reduction of sintering duration and process temperatures facilitating preservation of ceramic grains in nanoscale region [1-4].

In our preliminary work, we applied Rate-Controlled Sintering (RCS) technology to the SPS consolidation of the high melting point TiCN nanocomposites and investigated the influence of non-linear heating and loading regimes on the microstructure and properties formation process [3]. The current study is devoted to the SPS consolidation of high melting point TiN nanopowder as well as Si_3N_4-TiN and TiN-TiB_2 nanocompositions in non-linear regimes with the emphasis to exploration of microstructure and properties for consolidated materials. The selected compositions used in this study are commercially available on the market and widely used in industry.

2. Experimental methods

Titanium nitride (TiN) nanopowder (H.C. Stark GmbH, Germany) was used to estimate the influence of heating rate and pressure on powder sinterability and to develop a non-linear SPS regime. Silicon nitride (Si_3N_4) nanopowder (PCT ltd., Latvia) was used to prepare 50 wt.%TiN – 50 wt.% Si_3N_4 mixture. Si_3N_4 nanopowder used in this study was synthesized by ultra-rapid condensation from a gas phase together with Al_2O_3 and Y_2O_3, so the actual content of the silicon nitride in the powder was 86 wt% Si_3N_4 – 8wt% Al_2O_3 – 6wt.%Y_2O_3.

* IPMS, 3, KRZHIZHANOVSKY STR., 03680, KIEV, UKRAINE
** IKTS, WINTERBERGSTRASSE 28, D-01277, DRESDEN, GERMANY
*** WUT, WOŁOSKA 141, 02-507 WARSZAWA, POLAND
**** MRA LABORATORIES, INC., 15 PRINT WORKS DRIVE, ADAMS, MA, 01220, USA

The 50 wt.%TiN – 50 wt.% Si_3N_4 mixture was prepared by mechanical milling of the nanopowders in the planetary mill (Pulverizette 6, Fritsch, Germany) at 500 rpm during 4 hours in cyclohexane. In addition, plasma-chemically fabricated 80 wt.% TiN – 20 wt.%TiB_2 and 80wt.% TiN – 20wt% Si_3N_4 nanocompositions (PCT ltd., Latvia), were used to investigate SPS consolidation process and structure formation for composites prepared without mechanical milling.

Initial powder properties of the nanopowder compositions used in this study are summarized in Table 1. Transmissions Electron Microscopy (TEM) images of the initial nanopowders are presented on Fig. 1.

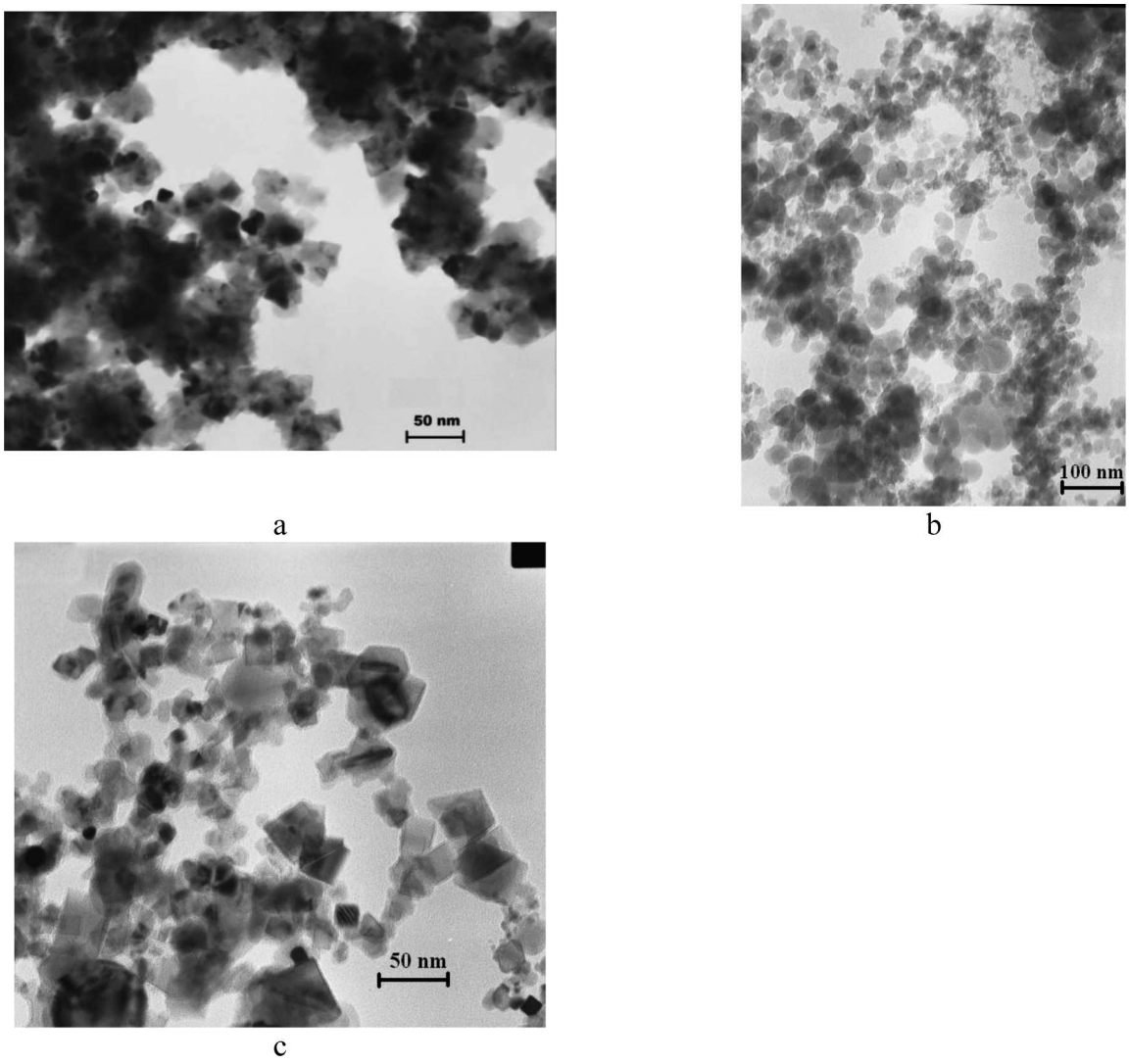

Fig. 1. TEM micrographs of the investigated nanostructured powders before processing: a – TiN nanopowder, b – Si_3N_4, c – TiN-20TiB_2

TABLE 1

Nanopowders and nanocompositions characterization

Nanopowder/ Nanocomposition	Producer	$d_{aver.}$, nm	Specific surface, m^2/g	[O], wt.%
TiN	HC Stark GmbH.	17	33	<1.5
TiN-20 wt%TiB_2	PCT ltd. Latvia	54	26	0.8
TiN - 20 wt%Si_3N_4	PCT ltd. Latvia	58	56	1.2
Si_3N_4 – 8wt%Al_2O_3– 6wt.%Y_2O_3	PCT ltd. Latvia	33	–	–

$d_{aver.}$ – average particle size estimated by laser granulometry.

SPS experiments had been carried out using SPS apparatus FCT-HP D 25 manufactured by FCT Systems GmbH (T_{max} = 2400 ^{0}C, P_{max} = 250 kN, I_{max} = 8000 A, U_{max} = 10 V, mediums: vacuum - 5· 10^{-2} mbar, nitrogen). All parameters were monitored during the experiments. The dilatation of powder samples during SPS consolidation process was monitored by recording of upper piston travel (the bottom piston was fixed). The dilatation data was then recalculated to the in situ sample densities. About 15 g of the nanopowder or nanocompositions were loaded into the graphite die (30 mm in diameter) followed by the application of 50 MPa pressure to establish a good contact between the powder sample and graphite pistons. Sintering experiments were organized according to the following procedure: TiN-based nanocomposites were SPS consolidated in a few stage regimes with sequential increase of pressure from 50 MPa to 70 MPa accompanied by the decrease of heating rate from 100°C /min to 20°C /min. An electric current was applied in a pulse mode with 20 ms pulse rate and 1 ms pause between pulses. The temperature was measured by a pyrometer on the inner surface of the upper graphite piston. The regimes used in the experiments are presented on the Fig. 2. No isothermal holding at the high temperatures were used to prevent uncontrolled grain growth.

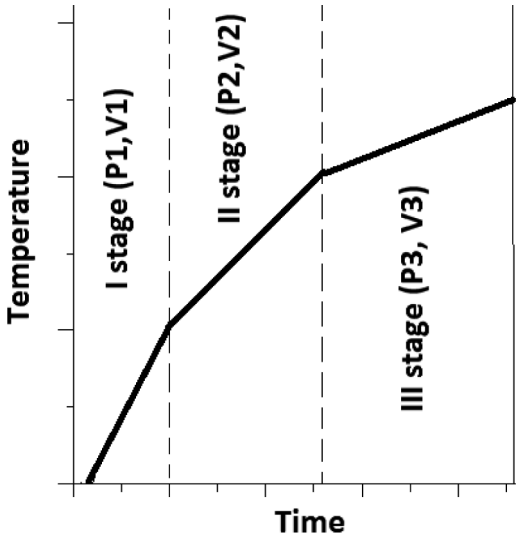

Fig. 2. Scheme of non-linear SPS regime for consolidation TiN-based nanopowders

3. Characterization

X-ray diffractometer (XRD – 7 with Cu Kα radiation, Seifert-FPM, Freiberg, Germany) was used for the qualitative phase analysis. Particle size distribution of the nanopowders was estimated using light scattering particle size analyzer (Zetasizer 1000 HS, Malvern Instruments, United Kingdom) and TEM microscope (JEOL JEM-2100F, Japan). Vickers hardness and fracture toughness of sintered composites were measured at 50g and 2 kg load conditions by MMT-3 (Buehler, USA) hardness tester. Nanohardness of consolidated nanomaterials was measured by a "Micron-Gamma" (National Aviation University, Ukraine) nanohardess tester using Berkovich indenter under 10g and 20g load conditions. Microstructure of the polished surface of sintered composites was examined by Field Emission Scanning Electron Microscope (NVision 40, Carl Zeiss SMT AG, Germany). High resolution microstructure observations were done using Scanning Transmission Electron Microscope (HD 2700, Hitachi, Japan) operated at 200 kV. Thin specimens for STEM observations were prepared by Focused Ion Beam system (FB 2100, Hitachi, Japan). Density of the SPS consolidated nanocomposites was measured by Archimedes method in deionised water at room temperature.

4. Results and discussion

4.1. Densification and structure formation of SPS sintered nanocomposites

A typical non-linear SPS process had been described in our preliminary work with TiCN [3]. A temperature-time profile of the non-linear SPS regime is presented on the Fig. 2. The regime includes three stages: i)initial stage with high heating rate(V_1), when about 75% of the material's density is achieved; ii) intermediate stage when the heating rate is partially decreased ($V_2<V_1$), and iii) final stage with slowest heating rate($V_3<V_2<V_1$). During the initial stage, a relatively low pressure is applied to the powder sample (P_1). In this stage, interactions between the particles play a decisive role. For conductive materials, for example, grow of the interparticle contacts leads to the increase of probability for electro-micro-discharges and facilitates acceleration of mass transfer compared to a conventional hot pressing process. During the next stage, higher pressures are applied to stimulate further densification of the specimen ($P_3>P_2>P_1$). In this case, the SPS process is controlled by the electric heating based on the Joule effect. The acceleration of the mass transfer in the SPS process leads to the decrease of sintering duration and temperature, and facilitates grains to remain in the nanoscale region.

First of all, we studied the densification of titanium nitride nanopowder, as basic component in compositions. Using the non-liner SPS regime with a peak temperature of 1200°C for consolidation of the TiN nanopowder, we were able to obtain fully dense 50 nm ceramic (Fig. 3a).

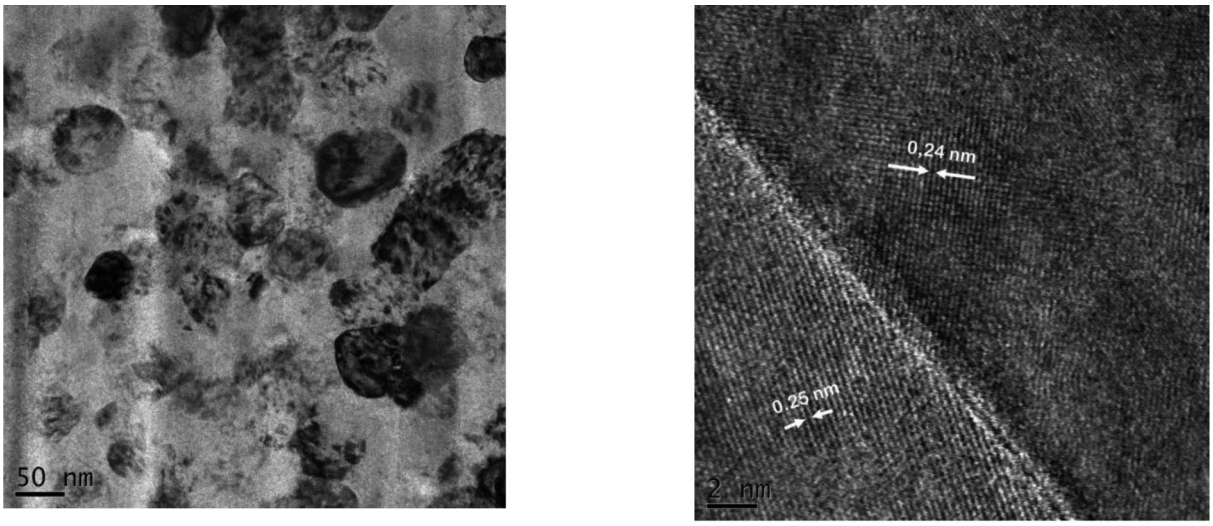

a B

Fig. 3. HR-STEM micrograph of nanostructured TiN powder after SPS consolidation in vacuum few step SPS to 1200 ?C: a – nanograins of TiN, b – grain boundary in nano-TiN consolidated material

Additionally, the grain boundary structure for nano-TiN powder consolidated under non-linear SPS regime has been investigated. The typical high-angle boundary between two TiN grains is presented on the fig 3b. As reported [4, 7] the main mechanisms of grain boundary formation for the bulk nanoceramics consolidated under SPS conditions are the dislocation-climb controlled route assisted by grain boundary sliding and local welding (conductive materials) for the samples sintered at a high-temperatures. In the case of non-linear SPS regime the grain boundaries formation preferably coming through diffusion-controlled conditions like in conventional presureless sintering [6]. Only the first stage of consolidation is controlled by particles rearrangement, while the following stages are controlled mostly by diffusion [3].

To verify the applicability of the multiple step SPS regime for a wider range of materials, we applied it to TiN – 20 wt%Si_3N_4, TiN – 50 wt%Si_3N_4 and TiN – 20 wt%TiB_2 nanocomposites. Several preliminary runs had been carried out to estimate densification rates, define process control temperatures and built multiple step SPS regimes. It was discovered that all compositions with high content of conductive components like TiN, TiB_2 demonstrate enhanced sinterability. The first composition, made from the electrically conductive phases, TiN – 20 wt%TiB_2, had been successfully densified into the nanograined ceramic using multiple step SPS regime with the peak temperature at 1470°C (Fig. 4). This ceramic exhibited fine homogeneous microstructure with average grain size below 100 nm. At the same time, the TiN-20Si_3N_4 composition was fully densified at 1300°C (Fig.5). Both compositions demonstrated

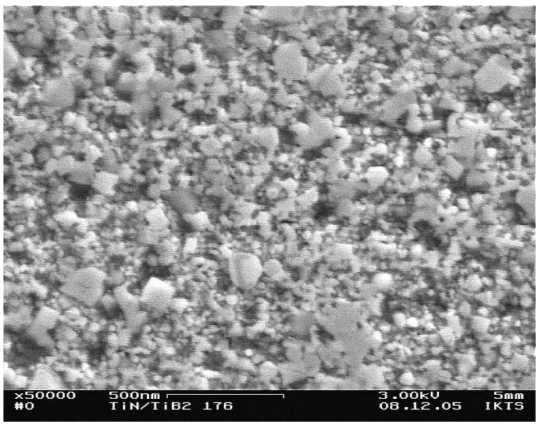

Fig. 4. FESEM micrograph of TiN – 20TiB_2 nanocomposition after few steps schedule SPS consolidation at 1470°C in nitrogen

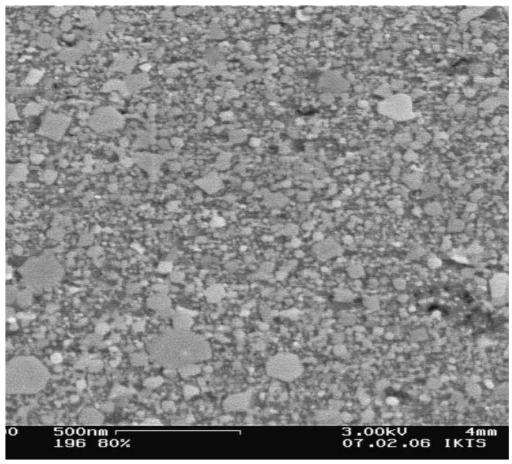

Fig. 5. FESEM micrograph of TiN-20Si_3N_4 nanocomposition after few steps schedule SPS consolidation at 1300°C in nitrogen

fine microstructure and low porosity. TiN-20 wt%Si_3N_4, however, revealed the formation of separate TiN grains with grain size around 200 nm. This may be the result of initial powder agglomeration or local overheating (welding) on the initial stage of sintering (Fig. 5). The ohmic resistivity of TiN -20 wt%TiB_2, TiN-20wt%Si_3N_4 composites and graphite is $\sim \cdot\ 10^{-8}$-$\cdot\cdot\ 10^{-7}\Omega$*m, $\sim \cdot\ 10^{-5}$- $10^{-4}\,\Omega\cdot$ m and $\sim 1,1\cdot\ 10^{-5}\Omega\cdot$ m respectively. The composition with higher resistivity (TiN-20wt%Si_3N_4) exhibited better sinterability in the SPS condition due to higher amount of Joule's heat.

Consolidation of composition TiN – 50 wt%Si_3N_4 doped by yttria and alumina has defined by the quantity of liquid phase formed at the temperatures 1400-1550°C. Formation of liquid phase starts at the temperature around 1400°C and promote densification process up to the peak temperature 1550°C. Usually, consolidation of the same composites with a high content of silicon nitride phase carry out at the temperatures as high as 1650°C [6]. Applying non-linear SPS process we control the quantity of liquid phase on the final stage of sintering *via* regulation of heating rate and additionally stimulate the densification by increasing of external pressure. Finally, composition TiN-50 wt%Si_3N_4 could be fully densified (99% of theoretical density) at the peak temperature 1550°C to homogeneous nanocomposite. Estimated grains size of components for composition TiN-50 wt%Si_3N_4 are: around 50 nm for grains of silicon nitride and 100-200 nm for TiN (Fig. 6). As discussed above, optimal peak temperature for titanium nitride to obtain dense ceramics with grains size around 50 nm is 1200°C. For composition with silicon nitride the temperature 1550°C is compromise between processes of

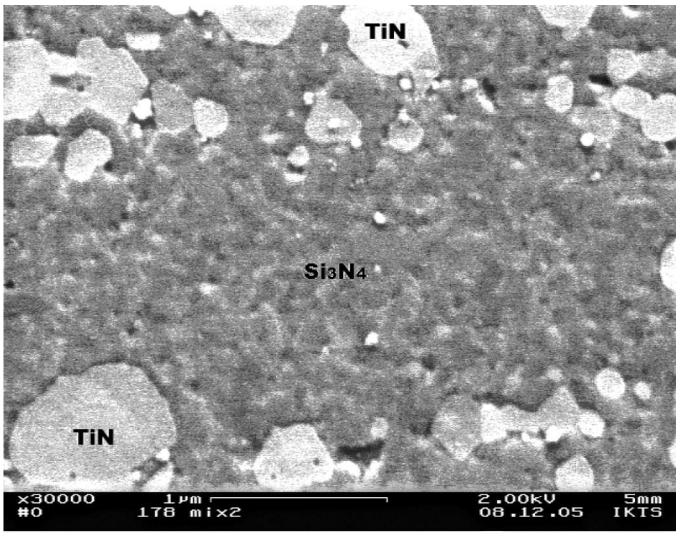

Fig. 6. Scanning electron microscope micrograph of TiN-50Si_3N_4 nanocomposition after few steps schedule SPS consolidation at 1600°C in nitrogen

composition densification and controlled grain growth of TiN nanoparticles in agglomerates.

4.2. Properties of nanocomposites

The consolidated materials were almost fully densified, so their mechanical properties were closely related to their microstructures (Tab. 2). Hardness of nanomaterials is strongly depends on the grain size and grain boundary width. On the micrometer scale, this improvement may not be significant. However, the reduction of grain size by a factor of two in the nanoscale region (e.g., from 100nm to 50 nm, or from 30nm to 15 nm) leads to a substantial increase of the absolute number of grain boundaries per volume, which affects the grain boundary-dependent properties.

We correlated theoretical ceramic hardness with grain size and grain boundary width for nanograined TiN ceramic via modified relationship of Hall-Petch (1) proposed in the work [8].

$$H = H_g \cdot (1 - -f) + H_{gb} \cdot f, \tag{1}$$

where H_g, H_{gb} – hardness of grains and grain boundaries, f – volume of grain boundaries.

Theoretically, estimated by the formula 1 maximal hardness in 32 GPa could be achieved for nano-TiN with grain size 10 nm. This size is critical size of pile-up dislocations existence in the grain [5,6]. It is a good evidence to start the work with TiN based nanocomposites and applies new technology to obtain nanograined ceramics with essentially enhanced hardness.

Practically, we calculate hardness of ~24 GPa for nano-TiN consolidated by SPS with grain size ~50 nm and grain boundary width ~1,02 nm. The data about grain size of TiN together with grain boundary width have been estimated from microstructure presented on the Fig. 3. The hardness value (24 GPa) was in a good agreement with our experimental data about nanohardness of TiN and mismatch with Vickers hardness data. Explanation of these differences could be explained by different volume of matter involved in tests. During nanoidentation only the surface matter are tested, at the same time for Vickers hardness tests (loads up to 10 kg) larger area of the specimens are under investigation.

Properties of few step SPS consolidated composites are summarized in Table 2.

TABLE 2

Properties of SPS consolidated composites

Composite (SPS in few stage schedule)	T_{final}, °C	Relative density, %	Fracture Toughness, MPa · $m^{1/2}$	Vickers Hardness, GPa	Nanohardness, GPa
TiN	1200	98.4	2.6	18.6±0.9	23.2±0.4
TiN - 20 wt%TiB_2	1470	98.7	4.1	22.5±2.1	32.1±0.8
TiN-20 wt%Si_3N_4	1300	98.1	5.3	20.3±1.8	25.8±0.9
TiN-50 wt%Si_3N_4	1550	99.0	5.5	19.5±1.9	22.6±0.9

As expected, the highest nanohardness (~32 GPa) was demonstrated by TiN-based composition with TiB_2 nanoparticles. In the composition TiB_2 is hardener and toughening phase (HV_{TiB2} ~34 GPa) which additionally work as inhibitor of TiN grain growth during SPS process. Moreover, uniformly distributed TiB_2 particles in nano-grained TiN matrix enhance fracture toughness of TiN – 20 wt%TiB_2 compositions up to the 4.1 MPa · $m^{1/2}$ compared with pure TiN nanoceramics.

For composition in the system TiN-Si_3N_4, TiN works as a hardening component, while Si_3N_4 increases fracture toughness of the matrerials.TiN-50 wt% Si_3N_4 composition showed relatively low nanohardness (~22 GPa), but good fracture toughness 5.5 MPa· $m^{1/2}$. For this composition, the main role plays "liquid phase", which forms between nanoparticles of main composition during sintering process. At the same time, composition TiN-20 wt%Si_3N_4 possessed most balanced configuration of components taking into account its properties (see Tab. 2). Furthermore, SPS consolidation of compositions in the systemTiN-Si_3N_4 without sintering aids additives like yttria and alumina is most perspective because processed at much lower temperatures compared with composites where "liquid phase" formed. In what follows, decreasing of sintering temperature for the TiN-Si_3N_4 composites is one of the important factors to refine grain size down to 10 nm and subsequently enhance mechanical properties for the materials.

5. Conclusions

Presented results prove the advantages of non-linear SPS process for consolidation of TiN based nanocomposites. High degree of densification together with fine microstructure (below 100 nm) could be achieved at relatively low temperatures for different types of ceramic composites via regulation of heating rate and process pressure on the final stages of consolidation. For example, 15 nm TiN nanopowder could be successfully SPS densified at 1200°C to a bulk 50 nm grain size nanocomposite. Moreover, TiN – TiB_2 and TiN-Si_3N_4 compositions could be successfully densified into the nanograined ceramics at the temperatures 150-300°C lower traditional SPS regimes without high temperature soaking. All SPS consolidated TiN-based nanocomposites demonstrated high mechanical properties: nanohardness 23-32 GPa and fracture toughness 4.1-5.5 MPa·$m^{1/2}$.

Acknowledgements

The authors wish to thank B.Weise and J. Raethel for his kind help regarding the experiments, K. Sempf N. Dubovitskaya and O. Butenko for their relevant technical support.

REFERENCES

[1] M. Nygren, Z. Shen, On the preparation of bio-, nano- and structural ceramics and composites by spark plasma sintering Solid State Sciences **5**, 125-131 (2003).
[2] J.R. Groza, A. Zavaliangos, Sintering activation by external electrical field, Mater. Sci. Eng. **A287**, 171-177 (2000).
[3] O. Zgalat-Lozynskyy, M. Herrmann, A. Ragulya, Spark plasma sintering of TiCN nanopowders in non-linear heating and loading regimes J. Europ. Ceram. Soc. **31**, 809-813 (2011).
[4] V.G. Kolesnichenko, et al., Field assisted sintering of nanocrystalline titanium nitride powder Powder Metallurgy and Metal Ceramics, 157-166 (2010).
[5] O. Zgalat-Lozynskyy, M. Herrmann, A. Ragulya, Nanostructured composites based on high-melting nitrides Silicon Industries 147-152 (2004).
[6] O. Zgalat-Lozynskyy, M. Herrmann, A. Ragulya, Nanostructured composites in the TiN-Si_3N_4 system, Proc. of the 10^{th} International Ceramics Congress (CIMTEC 2002), Part C- / Ed. P. Vincenzini. Techna Srl., 549-557 Faenza (2003).
[7] G. Bernard-Granger, et al., Spark plasma sintering of a commercially available granulated zirconia powder–II. Microstructure after sintering and ionic conductivity / Acta Materialia **56**, 4658-4672 (2008).
[8] D.A. Konstantinidis, E.C. Aifantis, On the anomalous hardness of nanocrystalline materials Nanostructured materials **7**, 1111-1118 (1998).

Received: 20 April 2012.